Early Earth zircons formed in residual granitic melts produced by tonalite differentiation

Oscar Laurent, Jean-François Moyen, Jörn-Frederik Wotzlaw, Jana Björnsen, Olivier Bachmann

Early Earth zircons formed in residual granitic melts produced by tonalite differentiation

Oscar Laurent[1,2], Jean-François Moyen[3], Jörn-Frederik Wotzlaw[1], Jana Björnsen[1] and Olivier Bachmann[1]

[1]ETH Zürich, Department of Earth Sciences, Clausiusstr. 25, 8092 Zürich, Switzerland

[2]CNRS, Géosciences Environnement Toulouse, 14 av. E. Belin, 31400 Toulouse, France

[3]Université de Lyon, Laboratoire Magmas et Volcans, 23 r. Dr. Paul Michelon, 42023 Saint Etienne, France

ABSTRACT

The oldest geological materials on Earth are Hadean (>4 Ga) detrital zircon grains. Their chemistry and apparently low Ti-in-zircon temperatures (≤700°C) are considered to be inconsistent with crystallization in a magma of the tonalite-trondhjemite-granodiorite (TTG) suite, although these are the dominant Archean (4.0–2.5 Ga old) silicic rocks. Using a new dataset of trace element contents in zircons from Paleoarchean Barberton TTGs (South Africa) and thermodynamic modelling, we show that these zircons have crystallized at near-solidus conditions from a compositionally uniform granitic melt. This melt is residual from the upper crustal crystallization of a less evolved (tonalitic) parent and thereby shows major and trace element compositions different from bulk TTG rocks. A global compilation reveals that most Hadean detrital and Archean TTG-hosted grains share a peculiar zircon trace element signature that is distinct from the chemical trends defined by Phanerozoic zircons. Our model shows that the low Ti contents of early Earth zircons reflect crystallization at higher temperatures (720–

800°C) than initially inferred, due to lower modelled TiO_2 activity in the melt relative to previous estimates. We therefore propose that near-solidus zircon crystallization from a chemically evolved melt in a TTG-like magmatic environment was the dominant zircon-forming process on the early Earth.

INTRODUCTION

The only remnants of the earliest felsic crust are Hadean (4.4–4.0 Ga-old) detrital zircon grains found in younger sedimentary rocks at Jack Hills, Western Australia (e.g. Harrison, 2020). Constraining the nature of the magma in which these zircons formed is key to understanding the geodynamic context of the early Earth. Although rocks of the tonalite-trondhjemite-granodiorite (TTG) suite dominate the earliest preserved Archean (4.0–2.5 Ga old) continental nuclei (Moyen, 2011), they have usually been discounted as potential parents for the Jack Hills zircons (e.g. Harrison, 2020). Specifically, the apparent crystallization temperatures of Jack Hills zircons (≤700 °C based on Ti-in-zircon thermometry; Watson and Harrison, 2005) are lower than those of TTG magma formation (>850 °C), and their trace element compositions do not seem to be in equilibrium with those of TTG bulk rocks (Rollinson, 2008; Reimink et al., 2020; Turner et al., 2020).

However, the study of zircon and zircon-hosted inclusions from a 3.81 Ga-old meta-tonalite from the Itsaq Gneiss Complex in Greenland showed that TTG magmas are initially zircon-undersaturated, so zircon should only crystallize at near-solidus conditions in residual granitic melts that formed after extensive cooling and crystallization (Nutman and Hiess, 2009). Moreover, changes in melt chemistry during crystallization may result in zircons forming from a melt showing significantly different trace element compositions than TTG bulk rocks. These

possibilities must be systematically addressed to evaluate whether TTG magmas could be plausible parents for Hadean detrital zircons.

For this purpose, we investigated the nature and composition of zircon-forming melts in TTG suites, based on new zircon trace element data from the Paleoarchean (3.46 Ga-old) TTGs of the Barberton area, Kaapvaal Craton, South Africa (Fig. 1). The compositional evolution of magmas in the course of crystallization, from the tonalitic starting compositions to the near-solidus granitic melts, is well constrained following a recent study (Laurent et al., 2020). The significance of the results is evaluated through a global comparison of Hadean and Archean zircons, based on a compilation of trace element compositions in Jack Hills detrital zircons (n = 233) and igneous TTG-hosted zircon (n = 947) in 44 samples from Archean cratons worldwide (Fig. 1A). Zircon compositions altered by the effects of radiation damage and/or post-magmatic (hydro-)thermal events were filtered out based on chemical and isotopic criteria from both newly acquired and compiled datasets. Details about data acquisition, compilation and filtering are provided in the Supplementary Material.

ZIRCON-FORMING MELTS IN ARCHEAN TTG SUITES

The 3.46 Ga Barberton TTGs consist of trondhjemite plutons with minor diorite, tonalite and granite; the plutons are associated with coeval and co-genetic felsic volcanic rocks of the Buck Ridge Volcanic Complex (Laurent et al., 2020) (Fig. 1B). The diverse igneous lithologies have been proposed to result from the differentiation of a parental liquid of tonalitic composition, whereby the compositional range of the plutonic rocks arises from various degrees of crystal accumulation and residual melt loss along the liquid line of descent (Fig. 1C).

Zircons from nine samples representative of the Barberton TTG suite show overlapping trace element concentrations (Fig. 2A and Supplementary Material, Fig. S1). In particular, Ti and Hf are powerful monitors of the crystallization environment of zircon, as Ti relates to the temperature and TiO_2 activity of the host melt (Ferry and Watson, 2007) and Hf is a proxy for melt fractionation (Claiborne et al., 2006). Although bulk-rock SiO_2 contents vary from ~60 to 76 wt%, zircon Ti and Hf concentrations in the Barberton samples show restricted ranges of 5.1 ± 3.2 ppm and 0.95 ± 0.17 wt.% (2 standard deviations [SD], n = 58) respectively (Fig. 2A). Similar observations were made from Phanerozoic igneous suites and interpreted as reflecting late crystallization of zircon from a compositionally homogeneous residual melt in all rock types, for instance in the Boggy Plain zoned pluton, southeastern Australia (Ickert et al., 2011). The observed distribution of zircon Ti and Hf concentrations in the Paleoarchean Barberton TTG plutons suggests a comparable situation.

The inversion of zircon compositions in the Barberton samples, using the parameterization of zircon/melt partition coefficients as a function of Ti concentration of Claiborne et al. (2018), further supports this interpretation. The composition of the calculated melts indeed overlaps with that of the high-silica granitic melt inclusions from the BRVC (Fig. 2B), which represent the most differentiated, residual melts from crystallization of the parent tonalitic magma (Laurent et al., 2020). Importantly, both the calculated melts and BRVC melt inclusions share the same distinctive differences with average TTGs, namely strikingly higher Th and U contents and a lower middle- to heavy rare earth element ratio (Fig. 2B). These features, which likely reflect the highly evolved nature of the melts and significant amphibole fractionation, explain the apparent disequilibrium between trace element concentrations of zircon and the composition of their host TTG rocks (Reimink et al., 2020).

We simulated the crystallization of the parental liquid of the Barberton TTG suite (as determined by Laurent et al., 2020) at 3 kbar, using the mineral and melt models of Holland et al. (2018) and the PERPLE_X software program (https://www.perplex.ethz.ch/; Connolly, 2009). The phase equilibria and thermodynamic data obtained served to model the evolution of melt Zr concentration as well as zircon saturation temperatures and Ti contents (see Supplementary Material for details). The results show a first step (from the liquidus at 1050 °C to ~40 wt.% liquid at 725 °C) of dominant plagioclase (~40 wt.%), subordinate amphibole (~15 wt.%), and minor pyroxene and Fe-Ti oxide crystallization (Fig. 3A). The melt fraction then decreases from 725 °C to the solidus (~700 °C), corresponding to the near-eutectic crystallization of quartz, plagioclase, K-feldspar and biotite. These results match the modal compositions recorded by natural samples (Laurent et al., 2020) and the experimental results of upper crustal tonalite crystallization (Marxer and Ulmer, 2019).

The low initial Zr content of the system (50–200 ppm), combined with buffering of the melt Zr concentration by amphibole crystallization, result in a range of zircon saturation temperatures (considering model uncertainties) between 800 °C and 720 °C (Fig. 3A). Zircon crystallizes in a high-silica residual melt similar to the BRVC melt inclusions in both major (Fig. 1C) and trace elements (Fig. 2B), which agrees with the observation of zircon in the interstitial domains between plagioclase and hornblende phenocrysts in natural samples (Laurent et al., 2020). These results are consistent with the inferred zircon crystallization temperatures (700–800°C) and granitic mineralogy of zircon-hosted inclusions in a 3.81 Ga-old tonalite from Greenland (Nutman and Hiess, 2009).

ZIRCON CRYSTALLIZATION CONDITIONS ON THE EARLY EARTH

Most TTG-hosted igneous zircons and many Jack Hills detrital zircons from our compilation compositionally overlap with the Paleoarchean Barberton zircons investigated here (Fig. 2A, 4 and Supplementary Material, Fig. S1). In Figure 4, we compared their Ti and Hf contents to those of zircon from various Phanerozoic igneous systems. Phanerozoic zircons show a negative correlation between Ti and Hf contents (Fig. 4) that reflects crystallization during magma cooling and differentiation (Claiborne et al., 2006). Such correlation may be recorded by zircons from single hand samples, as illustrated by one monzonite and one granite from the Miocene Spirit Mountain Batholith, southern Nevada, USA (Claiborne et al., 2006) (Fig. 4). In turn, distinct parental melt compositions and magma evolution pathways result in distinct zircon Ti-Hf co-variations for different geodynamic settings (Fig. 4).

In contrast, most early Earth zircons define a tight compositional cluster in the Ti-Hf space (Fig. 4) with very low Ti contents (2–9 ppm) (Carley et al., 2014) at moderate Hf concentrations (0.8–1.2 wt%). Strikingly, the variations in zircon Ti and Hf contents in the >40 early Earth samples taken together are more restricted than in single samples of the Spirit Mountain Batholith (Fig. 4). Although the early Earth zircons partly overlap with the compositionally most evolved, modern convergent margin and post-orogenic zircons, they clearly lack the high Ti (>15 ppm) and/or low Hf (<0.7 wt%) parts of the Phanerozoic trends (Fig. 4). Altogether, this supports the existence of specific conditions of zircon growth for Hadean and Archean zircons. As defined based on the Barberton case, these conditions are the crystallization from a near-solidus, residual granitic melt resulting from differentiation of a tonalitic parent magma, with little (if any) zircon fractionation having occurred beforehand. This condition may reflect the generally lower Zr concentrations of early Earth magmas (<150 ppm)

136 relative to Phanerozoic magmas (Keller et al., 2017), which would delay zircon saturation to
137 near-solidus temperatures.
138 This is confirmed by our crystallization model, in which zircon saturates only at ≤800 °C
139 and accordingly shows the low Ti concentrations (<10 ppm) (Fig. 3A-B) typical of early Earth
140 grains (Fig. 2A, Fig. 4). The modelled cumulative curve of Ti contents in zircon predicts a
141 greater proportion of low-Ti zircons than observed in nature (Fig. 3B). This may reflect that
142 during analysis of natural grains, thin zircon rims crystallized at low temperatures were
143 undersampled relative to large, higher-temperature cores (Ickert et al., 2011). However, the
144 observed concentration range is exactly the same (2–9 ppm Ti; Fig. 3B). This is a robust
145 indicator of the model's validity, as this range is controlled by zircon saturation temperature and
146 TiO_2 activity, which depend only on the initial Zr content of the liquid and phase relations during
147 crystallization. Importantly, the model indicates that the low Ti concentrations of the Jack Hills
148 zircons can be explained by crystallization at significantly higher temperatures (720–800 °C; Fig.
149 3B) than have been estimated so far (650–720 °C), because the TiO_2 activity of the system was
150 much lower (ca. 0.4–0.5 as modelled here) than was previously assumed for Ti-in-zircon
151 thermometry (up to 1; Watson and Harrison, 2005).
152
153 **CONCLUSIONS AND IMPLICATIONS**
154 We propose that (1) zircon in TTG suites forms at near-solidus temperatures (720–800
155 °C) from a residual granitic melt resulting from extensive crystallization of a tonalitic parent and,
156 hence, compositionally different from the bulk rocks; and (2) this zircon-forming mechanism is
157 common to all early Earth zircons, including the Jack Hills detrital grains, as shown by their
158 shared peculiar trace element signature that is distinct from that of Phanerozoic zircon. This

model reconciles the paradoxical observations that the low-Ti nature of the Jack Hills zircons (Watson and Harrison, 2005) reflects crystallization in a melt close to the granite minimum, although such granites are scarce in the early Earth (Moyen, 2011). This liquid may in fact be similar to the most differentiated melt of the TTG suites, which remained trapped in the crystalline framework and/or is not preserved as co-magmatic silicic volcanic rocks (Laurent et al., 2020).

Whether the Jack Hills zircons formed in voluminous TTG plutons, as observed in Archean cratons, or in lower-volume felsic veins and pods in a dominantly mafic crust (e.g. Rollinson, 2008) is still uncertain. In fact, the parameters controlling zircon chemistry, namely the petrogenesis of felsic magmas (intracrustal differentiation of hydrous mafic material) and hence their phase relationships upon crystallization, would be comparable in both cases. Nevertheless, closed-system crystallization as modelled here, which is more likely to occur in small, isolated melt pockets, may also explain the distributions of zircon Ti contents skewed to lower concentrations as compared to crystallization in large, open-system plutons (Fig. 3C). Interestingly, the compositional range of the Jack Hills zircons extends to lower Ti (1–3 ppm) and/or higher Hf (1.2–1.4 wt%) than that of the TTG-hosted zircons (Fig. 4), which may be explained by the smaller amounts of silicic melt and closed-system conditions, and/or even lower initial Zr contents, in the Hadean. Either way, our results indicate that the trace element composition of Hadean detrital zircons is consistent with a TTG-like magmatic environment.

ACKNOWLEDGMENTS

We thank M.P. Silva for help during data acquisition, and T. Johnson, A.P. Nutman and H. Rollinson for constructive reviews. This study was funded by the Swiss National Science

Foundation (grant 200021_178928 to OB) and the Australian Research Council (grant FL160100168 to JFM). This is International Research Project BuCoMo contribution A9.

REFERENCES CITED

Bell, E.A., Harrison, T.M., Kohl, I.E., Young, E.D., 2014. Eoarchean crustal evolution of the Jack Hills zircon source and loss of Hadean crust: Geochimica et Cosmochimica Acta, v. 146, p. 27–42.

Boehnke, P., Watson, E.B., Trail, D., Harrison, T.M., Schmitt, A.K., 2013. Zircon saturation re-revisited: Chemical Geology, v. 351, p. 324-334.

Bouvier, A.S., Ushikubo, T., Kita, N., Cavosie, A.J., Kozdon, R., Valley, J.W., 2012. Li isotopes and trace elements as a petrogenetic tracer in zircon: insights from Archean TTGs and sanukitoids: Contributions to Mineralogy and Petrology, v. 163, no. 5, p. 745–768.

Burnham, A.D., and Berry, A.J., 2017. Formation of Hadean granites by melting of igneous crust: Nature Geoscience, v. 321, p. 457–461.

Carley, T.L., Miller, C.F., Wooden, J.L., Padilla, A.J., Schmitt, A.K., Economos, R.C., Bindeman, I.N., Jordan, B.T., 2014, Iceland is not a magmatic analog for the Hadean: evidence from the zircon record: Earth and Planetary Science Letters, v. 405, p. 85–97.

Cavosie, A.J., Valley, J.W., Wilde, S.A., E.I.M.F., 2006. Correlated microanalysis of zircon: trace element, $\delta^{18}O$, and U–Th–Pb isotopic constraints on the igneous origin of complex >3900 Ma detrital grains: Geochimica et Cosmochimica Acta, v. 70, p. 5601–5616.

Claiborne, L.L., Miller, C.F., Gualda, G.A., Carley, T.L., Covey, A.K., Wooden, J.L., Fleming, M.A., 2018. Zircon as Magma Monitor: Robust, Temperature-Dependent Partition Coefficients from Glass and Zircon Surface and Rim Measurements from Natural

205 Systems, *in* Moser, D.E., Corfu, F., Darline, J.R., Reddy, S.M., and Tait, K., eds.,
206 Microstructural Geochronology: Planetary Records Down to Atom Scale (Geophysical
207 Monograph 232), John Wiley & Sons, p. 3–34.
208 Claiborne, L.L., Miller, C.F., Walker, B.A., Wooden, J.L., Mazdab, F.K., Bea, F., 2006.
209 Tracking magmatic processes through Zr/Hf ratios in rocks and Hf and Ti zoning in
210 zircons: an example from the Spirit Mountain batholith, Nevada: Mineralogical
211 Magazine, v. 70, p. 517–543.
212 Connolly, J.A.D., 2009. The geodynamic equation of state: what and how: Geochemistry
213 Geophysics Geosystems, v. 10, Q10014.
214 Ferry, J., Watson, E., 2007. New thermodynamic models and revised calibrations for the Ti-in-
215 zircon and Zr-in-rutile thermometers. Contributions to Mineralogy and Petrology: v. 154,
216 p. 429–437.
217 Grimes, C.B., John, B.E., Cheadle, M.J., Mazdab, F.K., Wooden, J.L., Swapp, S., Schwartz, J.J.,
218 2009. On the occurrence, trace element geochemistry, and crystallization history of
219 zircon from in situ ocean lithosphere: Contributions to Mineralogy and Petrology, v. 158,
220 p. 757–783.
221 Harrison, T.M., 2020. Hadean Jack Hills zircon geochemistry *in* Harrison, T.M., ed., Hadean
222 Earth: Springer, Cham, p. 143–178.
223 Holland, T.J., Green, E.C. & Powell, R. 2018. Melting of peridotites through to granites: a
224 simple thermodynamic model in the system KNCFMASHTOCr: Journal of Petrology, v.
225 59, p. 881–900.
226 Ickert, R.B., Williams, I.S., Wyborn, D., 2011. Ti in zircon from the Boggy Plain zoned pluton:
227 implications for zircon petrology and Hadean tectonics: Contributions to Mineralogy and

Petrology, v. 162, p. 447–461.

Karakas, O., Wotzlaw, J.F., Guillong, M., Ulmer, P., Brack, P., Economos, R.C., Bergantz, G.W., Sinigoi, S., Bachmann, O., 2019. The pace of crustal-scale magma accretion and differentiation beneath silicic caldera volcanoes: Geology, v. 47, no. 8, p. 719–723.

Keller, C.B., Boehnke, P., Schoene, B., 2017. Temporal variation in relative zircon abundance throughout Earth evolution: Geochemical Perspective Letters, v. 3, p. 179–189.

Kielman, R., Whitehouse, M., Nemchin, A., Kemp, A., 2018. A tonalitic analogue to ancient detrital zircon: Chemical Geology, v. 499, p. 43–57.

Kitajima, K., Ushikubo, T., Kita, N.T., Maruyama, S., Valley, J.W., 2012. Relative retention of trace element and oxygen isotope ratios in zircon from Archean rhyolite, Panorama Formation, North Pole Dome, Pilbara Craton, Western Australia: Chemical Geology, v. 332–333, p. 102–115.

Laurent, O., Björnsen, J., Wotzlaw, J.F., Bretscher, S., Pimenta Silva, M., Moyen, J.F., Ulmer, P., Bachmann, O., 2020. Earth's earliest granitoids are crystal-rich magma reservoirs tapped by silicic eruptions: Nature Geoscience, v. 13, p. 163–169.

Liu, J., Liu, F., Ding, Z., Liu, C., Yang, H., Liu, P., Wang, F., Meng, E., 2013. The growth, reworking and metamorphism of early Precambrian crust in the Jiaobei terrane, the North China Craton: Constraints from U–Th–Pb and Lu–Hf isotopic systematics, and REE concentrations of zircon from Archean granitoid gneisses: Precambrian Research, v. 224, p. 287–303.

Marxer, F., and Ulmer, P., 2019. Crystallization and zircon saturation of calc-alkaline tonalite from the Adamello Batholith at upper crustal conditions: an experimental study: Contributions to Mineralogy and Petrology, v. 174, 84.

Moyen, J.-F., 2011. The composite Archaean grey gneisses: Petrological significance, and evidence for a non-unique tectonic setting for Archaean crustal growth: Lithos, v. 123, no. 1–4, p. 21–36.

Nutman, A.P., Bennett, V.C., Friend, C.R.L., Horie, K., Hidaka, H., 2007. ~3,850 Ma tonalites in the Nuuk region, Greenland: geochemistryand their reworking within an Eoarchaean gneiss complex: Contributions to Mineralogy and Petrology, v. 154, p. 385–408.

Nutman, A.P., Hiess, J., 2009. A granitic inclusion suite within igneous zircons from a 3.81 Ga tonalite (W. Greenland): Restrictions for Hadean crustal evolution studies using detrital zircons: Chemical Geology, v. 261, p. 77–82.

Reimink, J.R., Davies, J.H.F.L., Bauer, A.M., Chacko, T., 2020. A comparison between zircons from the Acasta Gneiss Complex and the Jack Hills region. Earth and Planetary Science Letters: v. 531, 115975.

Rollinson, H., 2008. Ophiolitic trondhjemites: a possible analogue for Hadean felsic ‘crust’. Terra Nova: v. 20, p. 364–369.

Shan, H., Zhai, M., Wang, F., Zhou, Y., Santosh, M., Zhu, X., Zhang, H., Wang, W., 2015. Zircon U–Pb ages, geochemistry, and Nd–Hf isotopes of the TTG gneisses from the Jiaobei terrane: Implications for Neoarchean crustal evolution in the North China Craton: Journal of Asian Earth Sciences, v. 98, p. 61–74.

Turkina, O.M., Berezhnaya, N.G., Lepekhina, E.N., Kapitonov, I.N., 2012. U–Pb (SHRIMP II), Lu–Hf isotope and trace element geochemistry of zircons from high-grade metamorphic rocks of the Irkut terrane, Sharyzhalgay Uplift: Implications for the Neoarchaean evolution of the Siberian Craton: Gondwana Research, v. 21, p. 801–817.

Turner, S., Wilde, S., Wörner, G., Schaefer, B., Lai, Y.J., 2020. An andesitic source for Jack

Hills zircon supports onset of plate tectonics in the Hadean: Nature Communications, v. 11, 1241.

Vetrin, V.R., Belousova, E.A., Chupin, V.P., 2016. Trace Element Composition and Lu-Hf Isotope Systematics of Zircon from Plagiogneisses of the Kola Superdeep Well: Contribution of a Paleoarchean Crust in Mesoarchean Metavolcanic Rocks: Geochemistry International, v. 54, no. 1, p. 92–111.

Vezinet, A., Pearson, D.G., Thomassot, E., Stern, R.A., Sarkar, C., Luo, Y., Fisher, C.M., 2018. Hydrothermally-altered mafic crust as source for early Earth TTG: Pb/Hf/O isotope and trace element evidence in zircon from TTG of the Eoarchean Saglek Block, N. Labrador: Earth and Planetary Science Letters, v. 503, p. 95–107.

Watson, E.B., Harrison, T.M., 1983. Zircon saturation revisited: temperature and composition effects in a variety of crustal magmas types: Earth and Planetary Science Letters, v. 64, p. 295-304.

Watson, E.B., and Harrison, T.M., 2005. Zircon thermometer reveals minimum melting conditions on earliest Earth: Science, v. 308, p. 841–844.

Whitehouse, M.J., and Kamber, B.S., 2002. A rare earth element study of complex zircons from early Arcaean Amîtsoq gneisses, Godthåbsfjord, south-west Greenland: Precambrian Research, v. 126, p. 363–377.

Zong, K., Liu, Y., Zhang, Z., He, Z., Hu, Z., Guo, J., Chen, K., 2013. The generation and evolution of Archean continental crust in the Dunhuang block, northeastern Tarim craton, northwestern China: Precambrian Research, v. 235, p. 251–263.

FIGURE CAPTIONS

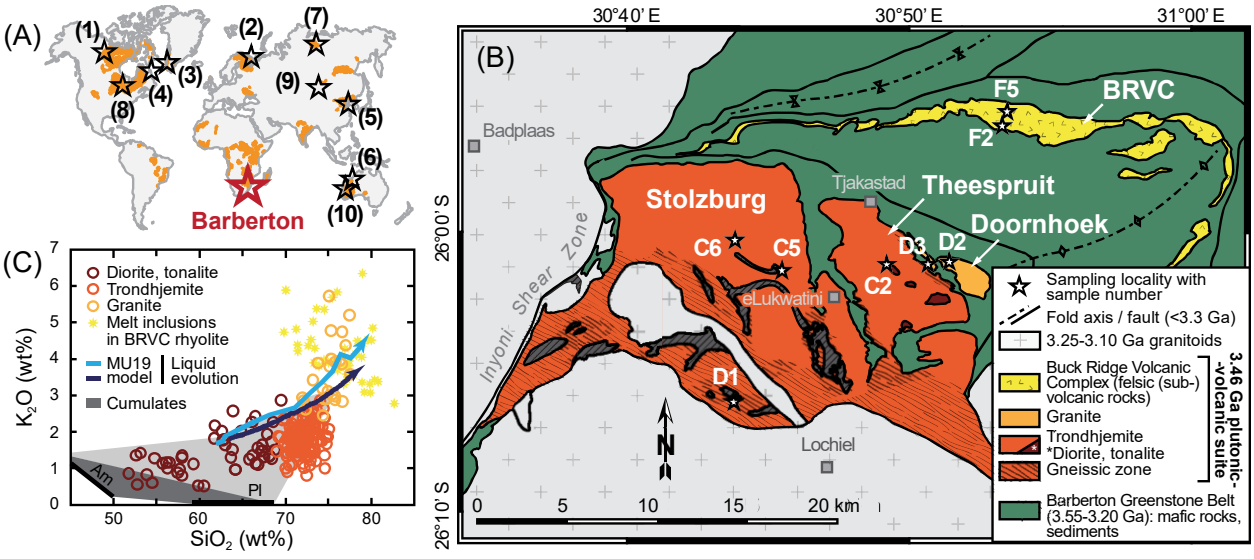

Figure 1. A: Location of zircon trace element data examined here: Barberton (this study); (1) Acasta Gneiss Complex (Reimink et al., 2020); (2) Kola (Vetrin et al., 2016); (3) Itsaq Gneiss Complex (Whitehouse and Kamber, 2002; Nutman et al., 2007; Kielman et al., 2018); (4) Uivak Gneiss (Vezinet et al., 2018); (5) Jiaobei Province (Liu et al., 2013; Shan et al., 2015); (6) North Pole Dome (Kitajima et al., 2012); (7) Irkut (Turkina et al., 2012); (8) Superior Province (Bouvier et al., 2012); (9) Tarim (Zong et al., 2013); (10) Jack Hills (Cavosie et al., 2006; Bell et al., 2014; Turner et al., 2020). B: Geological map of the Barberton Paleoarchean plutonic-volcanic suite, South Africa (Laurent et al., 2020); BRVC = Buck Ridge Volcanic Complex. C: K_2O vs. SiO_2 composition of bulk rock samples from the Barberton suite, BRVC melt inclusions and tonalite liquid lines of descent (experimental from Marxer and Ulmer, 2019 and modelled here – see text); the gray field represents mixed compositions between melts and plagioclase (Pl) + amphibole (Am) cumulates (adapted from Laurent et al., 2020).

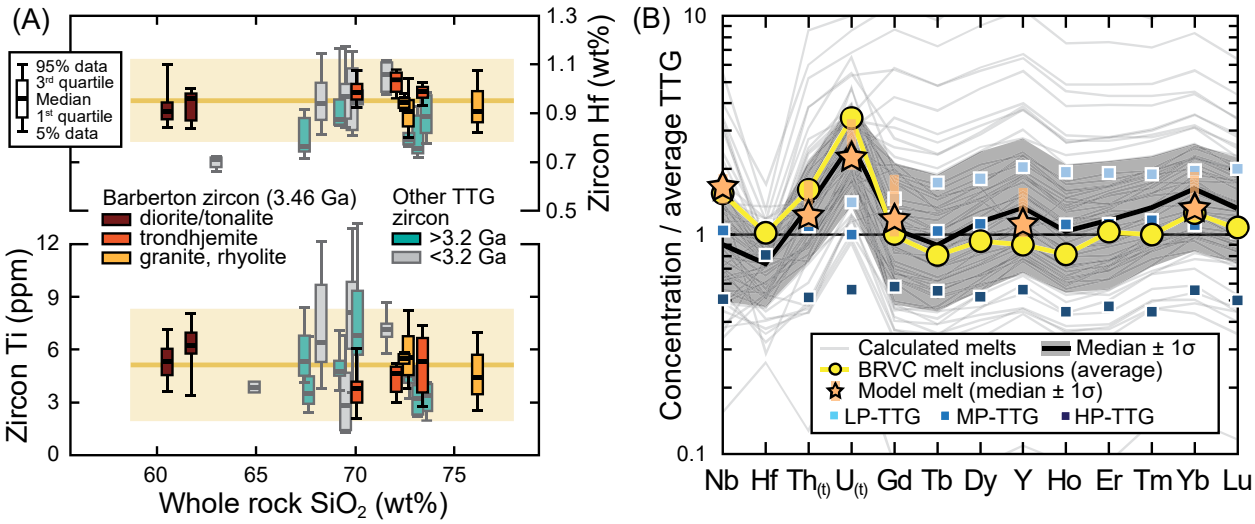

313

314 **Figure 2**. A. Plot of the distribution of zircon Ti and Hf contents in the Paleoarchean Barberton
315 and other Archean TTGs, as a function of the host rock SiO_2 content (one box-and-whisker per
316 sample). The horizontal lines and bands represent averages ± 2 SD of all Barberton zircons. B.
317 Trace element concentrations of zircon-forming melts (normalized to average TTG from Moyen,
318 2011) in the Barberton samples obtained from inversion of zircon compositions, compared to
319 those of the BRVC melt inclusions; the low-, medium- and high-pressure (LP-, MP-, HP-)TTG
320 groups (Moyen, 2011); and the melts saturating zircon in the crystallization model (see text). All
321 $Th_{(t)}$ and $U_{(t)}$ concentrations (including normalization values) are corrected for radioactive decay.

322

323

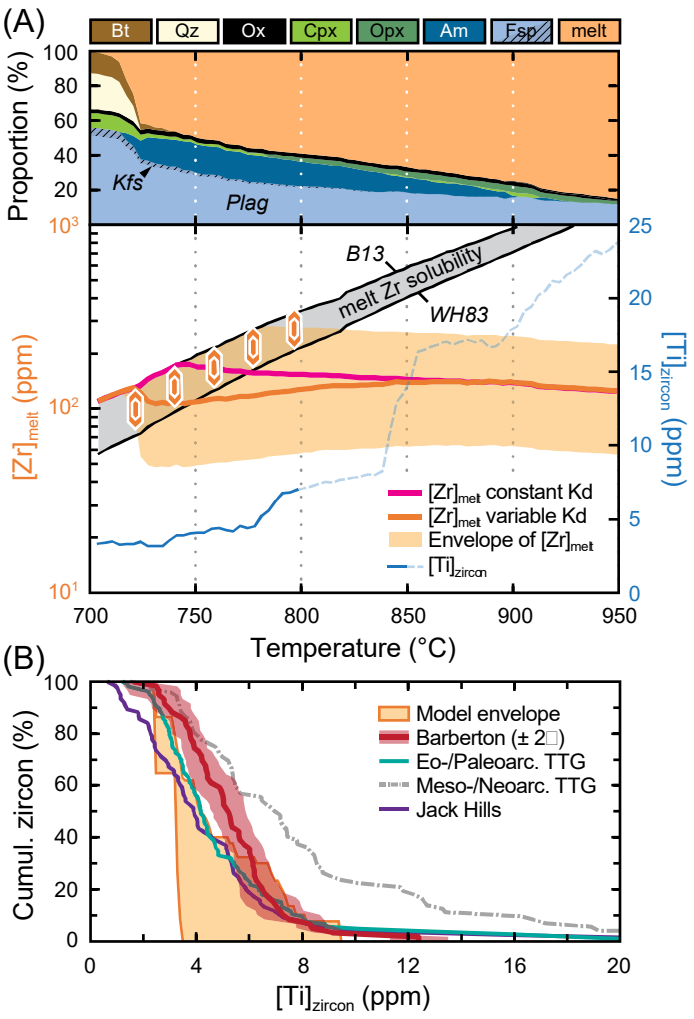

Figure 3. Results of the tonalite crystallization and zircon saturation model. A. Temperature evolution of phase proportions (top plot; Bt = biotite; Qz = quartz; Ox = Fe-Ti oxides; Cpx = clinopyroxene; Opx = orthopyroxene; Am = amphibole; Fsp = feldspar, including plagioclase [Plag] and K-feldspar [Kfs]); and modelled melt Zr content ($[Zr]_{melt}$, left axis) and zircon Ti concentrations ($[Ti]_{zircon}$, right axis) (bottom plot). Initial $[Zr]_{melt}$ ranges from 50 to 199 ppm (bounding the model envelope) with an average of 111 ppm (bold curves, obtained using either constant or variable Kd for Zr) (see details in Supplementary Material). The dashed curve shows theoretical $[Ti]_{zircon}$ at temperatures above zircon saturation. The melt Zr solubility range is bound by the models of Watson and Harrison (1983) (WH83) and Boehnke et al. (2013) (B13).

Zircon symbols represent the possible range of zircon saturation conditions within uncertainties. B. Cumulative proportions of $[Ti]_{zircon}$ in the model compared to early Earth TTG and Jack Hills zircons.

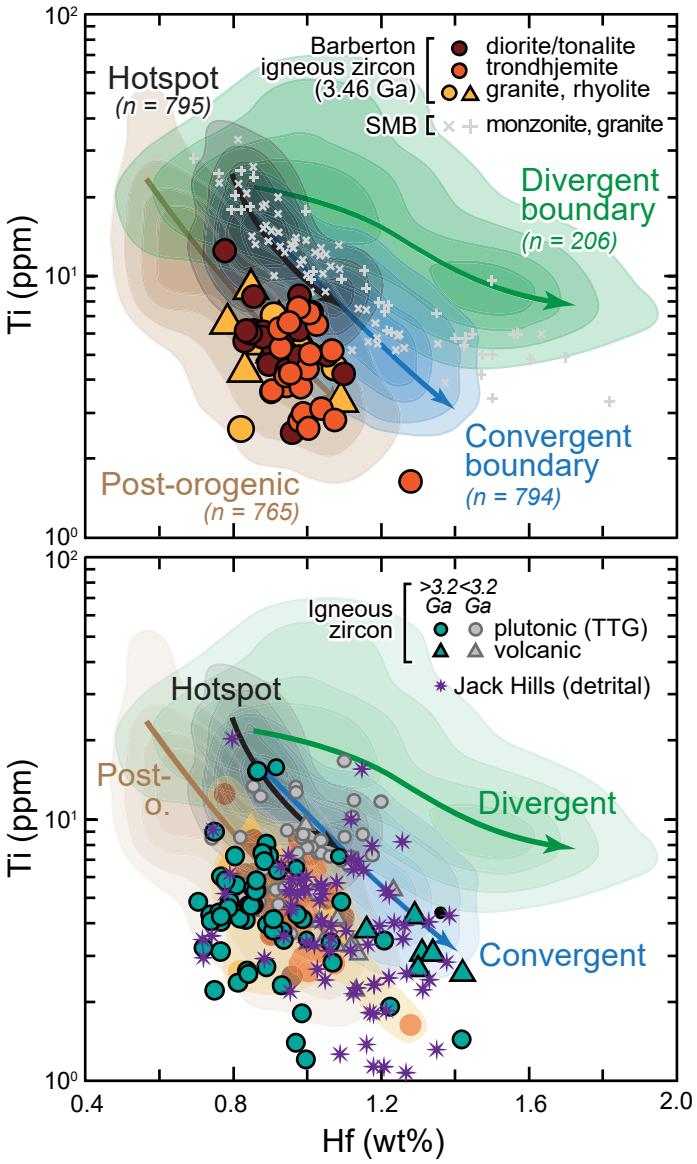

Figure 4. Titanium vs. Hf plots showing the composition of early Earth zircons and Phanerozoic zircons from different geodynamic settings (data from Burnham and Berry, 2017; Carley et al., 2014; Grimes et al., 2009; Karakas et al., 2019) as kernel density estimates contoured for 25, 50, 75 and 90% data; the arrows approximate the highest point density trends and correspond to the zircon compositional evolution throughout magma differentiation from mafic-intermediate to

345 felsic. The crosses depict zircon data from two samples (one monzonite, one granite) of the Spirit
346 Mountain Batholith (SMB) (Claiborne et al., 2006).
347
348
349 [1]GSA Data Repository item 202Xxxx, containing details about analytical and modelling
350 methods, data compilation, filtering, and zircon/melt partitioning, is available online at
351 www.geosociety.org/pubs/ft20XX.htm.